Extensive ground state entropy in supersymmetric lattice models

Hendrik van Eerten

Citation: J. Math. Phys. **46**, 123302 (2005); doi: 10.1063/1.2142836
View online: http://dx.doi.org/10.1063/1.2142836
View Table of Contents: http://aip.scitation.org/toc/jmp/46/12
Published by the American Institute of Physics

Extensive ground state entropy in supersymmetric lattice models

Hendrik van Eerten[a)]
Instituut voor Theoretische Fysica, Universiteit van Amsterdam, Valckenierstraat 65, 1018 XE Amsterdam, The Netherlands

(Received 22 September 2005; accepted 19 October 2005; published online 20 December 2005)

We present the result of calculations of the Witten index for a supersymmetric lattice model on lattices of various type and size. Because the model remains supersymmetric at finite lattice size, the Witten index can be calculated using row-to-row transfer matrices and the calculations are similar to calculations of the partition function at negative activity −1. The Witten index provides a lower bound on the number of ground states. We find strong numerical evidence that the Witten index grows exponentially with the number of sites of the lattice, implying that the model has extensive entropy in the ground state. © *2005 American Institute of Physics.* [DOI: 10.1063/1.2142836]

I. INTRODUCTION

In Ref. 1 a spinless fermion lattice model was proposed that is $N=2$ supersymmetric (SUSY) regardless of lattice size or shape. The (fine-tuned) Hamiltonian of this model is written in terms of fermion creation and annihilation operators, as follows:

$$H=\sum_i \sum_{j \text{ next to } i} P_{\langle i\rangle} c_i^\dagger c_j P_{\langle j\rangle} + \sum_i P_{\langle i\rangle}, \tag{1}$$

with i numbering the lattice sites, c_i and $c_i^\dagger$ obeying $\{c_i, c_j^\dagger\}=\delta_{ij}$ and where we have introduced *projection operators* P for convenient notation. The latter have the form

$$P_{\langle i\rangle} \equiv \prod_{j \text{ next to } i} (1-c_j^\dagger c_j). \tag{2}$$

These projection operators ensure that *no two neighboring sites can be occupied simultaneously*. Therefore, we will work with a restricted Hilbert space where these states are excluded.

The SUSY model is closely related to more conventional lattice models, like the Heisenberg *XXZ* chain. This relation, which holds if we take a one-dimensional (1D) chain with special boundary conditions for the lattice, was demonstrated in Ref. 2. There it was also shown how SUSY could aid a Bethe Ansatz computation of the spectrum of the *XXZ* chain. Indeed, it is fruitful to see how SUSY can facilitate calculations on the lattice model specified by (1), especially since the symmetry holds on arbitrary graphs while exact results on higher dimensional lattices are notoriously difficult to obtain using conventional methods.

The supersymmetry can be viewed as a multiple site generalization of supersymmetric quantum mechanics. The two generators Q^+ and Q^- are given explicitly in Ref. 1,

a)Electronic mail: hveerten@science.uva.nl

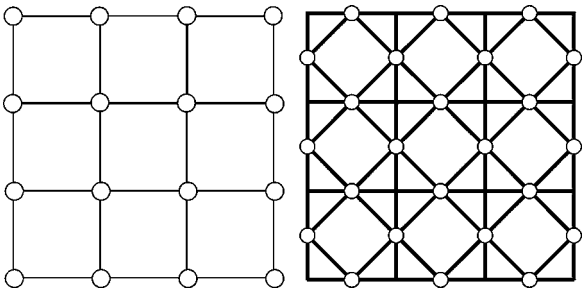

FIG. 1. The square lattice and the square dimer lattice.

$$Q^+ = \sum_{i=1}^{N} c_i^\dagger P_{\langle i \rangle}, \quad Q^- = \sum_{i=1}^{N} c_i P_{\langle i \rangle}. \tag{3}$$

We have the following algebraic structure (with F the fermionic number operator):

$$[F, Q^\pm] = \pm Q^\pm, \quad [F, H] = 0, \quad [Q^+, H] = 0, \quad [Q^-, H] = 0, \quad \{Q^+, Q^-\} = H. \tag{4}$$

In this paper we will focus on the ground states of a variety of two-dimensional (2D) lattices. We will treat the triangular and hexagonal lattice and their counterparts with dimer configurations as well as the dimer version of the square lattice. The square lattice was treated in a separate presentation.[3] All the lattices treated here have an interesting common feature, the number of ground states of the SUSY Hamiltonian on these lattices increases exponentially with increasing lattice size. This directly implies an extensive entropy of the ground state, a rare property exhibited by only a few condensed matter systems. The lattices are shown in Figs. 1–3.

All excited states in the SUSY model occur pairwise, because for every bosonic configuration we have an accompanying fermionic configuration. Here, lattice configurations with an even (odd) number of fermions are termed bosonic (fermionic) configurations. The ground states need not occur pairwise but are restricted otherwise, for their energies are all zero. All this means that we can use the Witten index operator to obtain a lower limit on the number of ground states,

$$W = \mathrm{Tr}(-1)^F e^{-\beta H}. \tag{5}$$

The pairwise cancelling of all excited states allows us to look just at the limiting case $\beta \to 0$, especially when calculating W for finite size lattices where convergence is not an issue, and we will do so for the remainder of this paper.

The operator W is completely equivalent to the well-known grand canonical partion function $Z = \mathrm{Tr}\, z^F \exp(-\beta H)$ of the classical hard particle model in the same dimension, only with a *negative* value for the activity z. It is this equivalence that puts a calculation of the Witten index for SUSY lattice models in a broader context and allows us to use well-known approaches for the

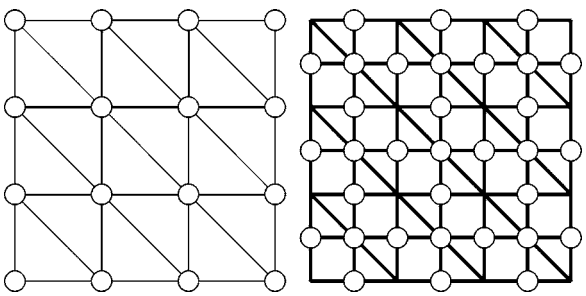

FIG. 2. The triangular lattice and the triangular dimer lattice.

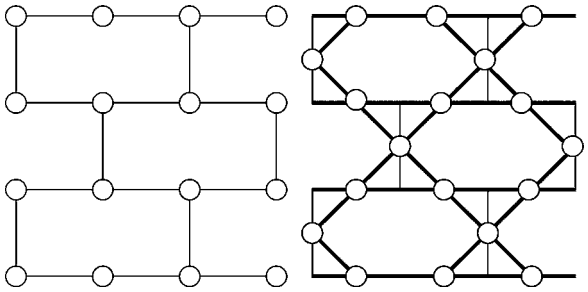

FIG. 3. The hexagonal lattice and the hexagonal dimer lattice.

calculation of Z—especially the use of *transfer matrices* that allows us to write W as the trace of a matrix product.

We have calculated the Witten index for finite sized lattices up to 15×15 (the triangular lattice) using transfer matrices. Before discussing the resulting values for the Witten indices, we will first explain how these matrices were constructed.

II. THE TRANSFER MATRICES

Transfer matrices can be constructed in various ways, as long as they provide a means of systematically summing over all possible configurations on the lattice (see Ref. 4 for an exhaustive introduction). For the N-site chain with periodic boundary conditions, the Witten index operator can be written in terms of transfer matrices as

$$W=\mathrm{Tr}\begin{pmatrix}1 & i\\ i & 0\end{pmatrix}^N=\mathrm{Tr}\begin{pmatrix}1 & -1\\ 1 & 0\end{pmatrix}^N. \tag{6}$$

The upper left entry of the matrix corresponds to adding an empty site to the chain with an empty site at the end, the upper right entry to adding a filled site to an empty site, the lower left entry to adding an empty site to a filled site and the lower right entry to adding a filled site to a filled site. This last entry must be zero because no configurations with neighboring sites filled were allowed. To avoid an overcounting per fermion we can either use $-1,1$ or i,i for the off-diagonal entries, as long as their product is equal to -1. The resulting transfer matrices can be made symmetric, but never Hermitian.

The procedure can easily be generalized to higher dimensional lattices. The easiest strategy is to use row-to-row transfer matrices and have each matrix entry correspond to a specific row configuration. Because the size of these matrices increases fast with increasing lattice size, the actual constructions of the matrices are best left to a computer (which we did). In the following, we will briefly explain how the matrices were constructed for the various lattices.

The square lattice is the simplest. For each matrix entry (i,j) the computer program just compares the configuration denoted by i with the one denoted by j. The matrix entry will be zero if the two configurations have one or more neighboring vertices occupied when viewed next to each other. If the combination of i and j is allowed, a factor $(-1)^{f(j)}$ is written down, where $f(j)$ stands for the number of fermions in configuration j. This means we obtain a non-symmetric matrix with real numbers only. Using a mapping from the different configurations to binary numbers simplifies matters even further (e.g., ● ○ ● ○ ○→10 100, etc.). The comparison between the ith and jth configuration can now be performed using a binary AND instruction.

The program is easily modified for the triangular lattice. There are two extra edges per vertex connecting to vertices on a higher or lower row. They are similar to the vertical edge, but with all vertices of the lower row shifted one position to the right. In terms of the computer code, when comparing the ith and jth configuration, we apply a binary right shift on the jth binary representation before using AND. The program now performs two tests instead of one to ascertain if it can enter a nonzero value.

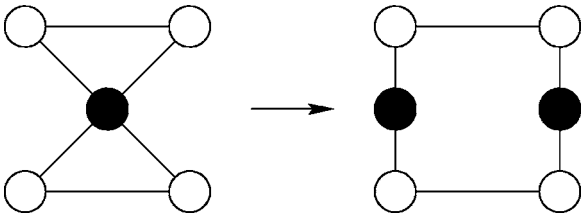

FIG. 4. Doubling sites on the even rows of the hexagonal dimer lattice.

For the hexagonal lattice we need to use two transfer matrices instead of one. Viewing the hexagonal lattice as a horizontal brick wall, we see that we have two different rows. If we work in units of 2×2 sites, we can take the transfer matrix that adds two rows at once as the matrix product of the two different matrices of the single rows.

The dimer lattices offer another complication. The square dimer lattice has both horizontal and vertical dimers. When constructing the transfer matrix we will sum over the horizontal dimer contributions. We can do this without problems because the horizontal dimers make no contact with the next row. For the triangular dimer lattice, we calculate the transfer matrices in a similar way.

For the hexagonal dimer lattice we will use yet another trick. As can be seen in Fig. 3, the even rows contain only half the number of vertices (after switching dimers and vertices in the original hexagonal lattice). As a first step we shall double this number of vertices in the even rows, as shown in Fig. 4. We must make certain that the resulting pairs consistently have the same value. Then we can formulate the transfer matrix once more as the product of two transfer matrices.

III. RESULTS

The resulting values for the Witten index on various lattice sizes are summarized in the tables in the Appendix.

The Witten index for the $M\times N$ lattice is given by Tr $(\mathbf{T}_N)^M$. Because we are taking the trace, the transfer matrices can be diagonalized without changing the resulting value for the Witten index. As a consequence, in the limiting case where the number of rows goes to infinity we can restrict ourselves to the largest roots of the characteristic polynomial of $\mathbf{T}_N$ (we would have used the term *eigenvalue* if the transfer matrix was not defective). Because the characteristic roots turn out to come in complex pairs, we must look at *two* largest roots and we get the following approximation for the Witten index:

$$W_{M,N} \approx a(t_{1,N})^M + \bar{a}(\bar{t}_{1,N})^M, \tag{7}$$

where $t_{1,N}$ and $\bar{t}_{1,N}$ denote the complex pair that form the largest roots of the N-column transfer matrix.

We can define a *contribution per site w* by

$$w \equiv \lim_{N\to\infty} \frac{t_{1,N}}{t_{1,N-1}}. \tag{8}$$

If we do not take the limit to infinite N, but study finite size lattices of increasing size, we find strong numerical evidence that the contribution to the Witten index per site rapidly tends to a fixed complex number that is different for each lattice that was considered. These numbers are shown in Table I. When calculating these numbers we must select the correct phase factors manually from the two possibilities offered by the complex pairs. The quickly appearing convergence to a fixed value then justifies our choice. The square lattice is treated elsewhere,[3] but has the special property that all characteristic roots have norm equal to 1. All other lattice types have a single complex pair of largest roots.

This convergence to a complex number greater than 1 has an important consequence, for it

TABLE I. Witten index per site, various lattice types.

Lattice type	Modulus $\|w\|$ per site	Phase $\arg w$ per site
Square dimer	1.33 ± 0.01	$(0.363 \times \pi) \pm 0.01$
Triangular	1.14 ± 0.01	$(0.178 \times \pi) \pm 0.01$
Triangular dimer	1.261 ± 0.01	$(0.189 \times \pi) \pm 0.001$
Hexagonal	1.2 ± 0.1	Insufficient data
Hexagonal dimer	1.4 ± 0.1	$(0.310 \times \pi) \pm 0.001$

indicates an *extensive ground state entropy*. The Witten index can by approximated by

$$W \approx w^{MN} + \bar{w}^{MN} = 2r^{MN} \cos(MN\theta + \theta_0), \tag{9}$$

with $w = r \exp[i\theta]$. The index provides a lower bound on the number of ground states. [Indeed it is very well possible that the actual number of ground states greatly exceeds $|W|$. The reasoning presented here offers us no information on this. See Refs. 3 and 6 for an example (the square lattice).] In our understanding the oscillating (cosine) factor is due to partial cancelations in W of contributions coming from bosonic and fermionic ground states. We thus expect that the monotonically growing factor r^{MN} sets a lower bound for the actual ground state entropy $S_0 \equiv \ln[\#\text{ground states}]$ according to

$$S_0 \geqslant MN \ln r. \tag{10}$$

For example, for the triangular lattice we find

$$S_0 \geqslant MN \ln 1.14 = 0.131MN. \tag{11}$$

It is interesting to see whether the Witten index per site can be calculated analytically. The triangular lattice case, for example, is equivalent to the hard hexagon model (see Ref. 5) with activity -1 and even fits the Yang-Baxter equation at this value. Unfortunately one cannot simply modify the reasoning from Ref. 4 for the $z<0$ regime because the transfer matrices are defective, so this question remains open for the moment. It might still be possible to obtain analytical solutions using other methods. In Ref. 6, for example, an exact solution for the nonagon-triangle lattice was found by showing that it is equivalent to the number of closed packed dimer coverings on the honeycomb lattice.

The fact that we have a complex number indicates that the Witten index does not necessarily grow with increasing lattice size, like the partition sum of the corresponding hard particle model in the $z>0$ regime would. The phase factor can be used to obtain a rough first estimate on the fermion density of the ground states. The phase factor in the cosine term of W shows us how many sites we need to add to get from a majority of fermionic ground states to a majority of bosonic ground states and vice versa. [For example, the 1D chain has roots $\exp(\pm i/3\pi)$ and only two ground states both with filling factor $1/3$]. But it is only useful as such when combined with a more advanced approach to calculating the spectrum like the spectral sequence technique used in Ref. 3. After all, the phase factor is determined by *all* ground states and they do not necessarily all have the same filling factors.

ACKNOWLEDGMENTS

The author wishes to thank Paul Fendley for helpful discussions and Kareljan Schoutens for careful reading of the paper.

APPENDIX: WITTEN INDEX TABLES

The hexagonal lattice tables correspond to the vertical brick wall. It has been confirmed that the tables for the horizontal brick wall are equal to the transposed tables. (See Tables II–VIII.)

TABLE II. Witten index for $M \times N$ square dimer lattice.

	1	2	3	4	5
1	1	−1	−2	−1	1
2	−1	1	8	−15	19
3	−2	8	−26	44	−92
4	−1	−15	44	129	−361
5	1	19	−92	−361	−2344
6	2	4	188	−912	−9158
7	1	−57	−338	4479	−24 219
8	−1	129	572	4417	−8241
9	−2	−136	−818	−46 612	362 068
10	−1	−39	668	5665	2 617 744

TABLE III. Witten index for $M \times N$ square dimer lattice (continued).

	6	7	8	9	10
1	2	1	−1	−2	−1
2	4	−57	129	−136	−39
3	188	−338	572	−818	668
4	−912	4479	4417	−46 612	5665
5	−9158	−24 219	−8241	362 068	2 617 744
6	−54 584	−239 790	−630 384	1 243 052	31 152 804
7	−239 790	1 495 453	9 803 807	−95 946 944	−363 241 257
8	−630 384	9 803 807	−130 406 911	1 458 639 932	−1 665 351 583
9	1 243 052	−95 946 944	1 458 639 932	−980 392 698	−436 754 324
10	31 152 804	−363 241 257	−1 665 351 583	−436 754 324	1 741 554 048

TABLE IV. Witten index for $M \times N$ triangular lattice.

	1	2	3	4	5	6	7	8	9	10
1	1	1	1	1	1	1	1	1	1	1
2	1	−3	−5	1	11	9	−13	−31	−5	57
3	1	−5	−2	7	1	−14	1	31	−2	−65
4	1	1	7	−23	11	25	−69	193	−29	−279
5	1	11	1	11	36	−49	211	−349	811	−1064
6	1	9	−14	25	−49	−102	−13	−415	1462	−4911
7	1	−13	1	−69	211	−13	−797	3403	−7055	5237
8	1	−31	31	193	−349	−415	3403	881	−28 517	50 849
9	1	−5	−2	−29	881	1462	−7055	−28 517	31 399	313 315
10	1	57	−65	−279	−1064	−4911	5237	50 849	313 315	950 592
11	1	67	1	859	1651	12 607	32 418	159 083	499 060	2 011 307
12	1	−47	130	−1295	−589	−26 006	−152 697	−535 895	−2 573 258	−3 973 827
13	1	−181	1	−77	−1949	67 523	330 331	−595 373	−10 989 458	−49 705 161
14	1	−87	−257	3641	12 611	−139 935	−235 717	5 651 377	4 765 189	−232 675 057
15	1	275	−2	−8053	−32 664	272 486	−1 184 714	−1 867 189	134 858 383	−702 709 340

TABLE V. Witten index for $M \times N$ triangular lattice (continued).

	11	12	13	14	15
1	1	1	1	1	1
2	67	−47	−181	−87	275
3	1	130	1	−257	−2
4	859	−1295	−77	3641	−8053
5	1651	−589	−1949	12 611	−32 664
6	12 607	−26 006	67 523	−139 935	272 486
7	32 418	−152 697	330 331	−235 717	−1 184 714
8	159 083	−535 895	−595 373	5 651 377	−1 867 189
9	499 060	−2 573 258	−10 989 458	4 765 189	134 858 383
10	2 011 307	−3 973 827	−49 705 161	−232 675 057	−702 709 340
11	5 102 879	12 409 123	18 205 045	−129 877 296	−1 457 956 169
12	12 409 123	232 286 890	1 851 105 439	1 476 815 313	−1 132 095 426
13	18 205 045	1 851 105 439	−1 938 183 221	1 466 459 831	1 016 873 233
14	−129 877 296	1 476 815 313	1 466 459 831	139 861 123	−1 366 302 204
15	−1 457 956 169	−1 132 095 426	1 016 873 233	−1 366 302 204	1 417 898 645

TABLE VI. Witten index for $M \times N$ triangular dimer lattice.

	2	4	6	8	10	12	16	18
2	1	−3	−5	1	11	9	−13	−31
4	−3	1	21	−79	157	−71	−731	3105
6	−5	21	−44	−47	995	6576	32 279	−131 167
8	1	−79	−47	3329	3801	−134 959	−217 671	5 439 681
10	11	157	995	3801	−37 009	−1 110 731	−17 397 663	−217 844 591
12	9	−71	−6576	−134 959	−1 110 731	11 324 392	538 444 825	105 699 937
14	−13	−731	32 279	−217 671	−17 397 663	538 444 825	−600 643 992	−914 519 359
16	−31	3105	−131 167	5 439 681	−217 844 591	105 699 937	−914 519 359	

TABLE VII. Witten index for $M \times N$ hexagonal lattice.

	2	4	6	8	10	12	14	16	18
2	−1	−1	2	−1	−1	2	−1	−1	2
4	3	7	18	47	123	322	843	2207	5778
6	−1	−1	32	−73	44	356	−1387	2087	2435
8	3	7	18	55	123	322	843	2215	5778
10	−1	−1	152	−321	−171	7412	−26 496	10 079	393 767
12	3	7	156	1511	6648	29 224	150 069	1 039 991	6 208 815
14	−1	−1	338	727	−5671	1850	183 560	−279 497	−4 542 907
16	3	7	1362	12 183	31 803	379 810	5 970 107	55 449 303	327 070 578

TABLE VIII. Witten index for $M \times N$ hexagonal dimer lattice.

	2	4	6	8	10	12	14	16
2	0	−8	0	32	0	−128	0	512
4	−4	8	32	−224	896	−2176	1536	16 896
6	12	88	576	3296	17 472	77 056	194 304	−1 139 200
8	4	−496	−3056	118 912	1 287 744	−25 732 864	−439 656 192	626 526 208
10	−40	1832	−42 400	1 088 352	−19 939 840	205 139 072	−878 495 232	1 612 654 080
12	44	−2872	−425 344	−23 115 488	84 888 704	420 235 264	335 598 080	−1 677 852 160
14	84	−12 440	−3 459 792	−336 941 664	−936 816 704	1 524 979 328	1 080 971 264	1 869 085 184

[1] P. Fendley, K. Schoutens, and J. de Boer, Phys. Rev. Lett. **90**, 120402 (2003).
[2] P. Fendley, K. Schoutens, and B. Nienhuis, J. Phys. A **36**, 12399 (2003).
[3] P. Fendley, K. Schoutens, and H. van Eerten, J. Phys. A **38**, 315 (2005).
[4] R. J. Baxter, *Exactly Solved Models in Statistical Mechanics* (Academic, London, 1982).
[5] R. J. Baxter, J. Phys. A **13**, L61 (1980).
[6] P. Fendley and K. Schoutens, Phys. Rev. Lett. **95**, 046403 (2005).